

Ab Initio SCF Calculations on the Photochemical Behavior of the Three-Membered Rings. 3. Oxirane: Ring Opening¹

B. Bigot, A. Sevin, and A. Devaquet*

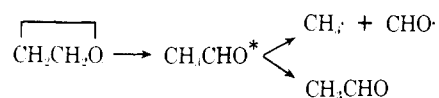
Contribution from the Laboratoire de Chimie Organique Théorique,² Université Pierre et Marie Curie, 4, Place Jussieu, 75230 Paris Cedex 05, France. Received May 30, 1978

Abstract: In this paper and the accompanying one the overall thermal and photochemical behavior of oxiranes is theoretically simulated with ethylene oxide as a prototype. An ab initio SCF method (STO-3G basis) followed by a limited CI involving the first 100 mono- and biexcited configurations is used in order to provide a basis for a semiquantitative rationale of the main reactive trends. Primary processes are examined in a first part: ring cleavage by CO bond rupture and different types of CC bond cleavage (the face to face, the conrotatory, and the disrotatory modes).

For a long time, oxirane derivatives have been used as key intermediates in the synthesis of a great variety of organic compounds.³ In solution, their chemical reactions involve electrophilic as well as nucleophilic attacks. However, aside from this behavior, oxiranes can undergo monomolecular thermal or photochemical reactions leading to various ring openings and fragmentations. Experimentally, this field is still growing,⁴ although it has already been abundantly studied.⁵

A recent study by Kawasaki,^{4a} whose results are summarized in Table I, makes conspicuous the following facts for ethylene oxide: (1) whatever the conditions, the major reaction is formation of two radical fragments ($\text{CH}_3\cdot$ and $\text{CHO}\cdot$); (2) photochemically, formation of atomic oxygen and ethylene increases at short wavelength while the preceding fragmentation is favored by a red shift of the irradiation wavelength; (3) sensitization increases the amount of stable acetaldehyde.

The common postulated intermediate^{6a} of these reactions is a "hot" acetaldehyde, which has been detected,^{6b} according to the scheme



The activation energy for the formation of CH_3CHO^* is 57 kcal/mol and its lifetime is $10^{-8.5}$ s at 400–500 Torr.^{6b} It appears that, photochemically as well as thermally, the reactive pathway always involves CO cleavage as primary process.

For substituted oxiranes, a dichotomy arises since this time both CC and CO bonds can be broken depending on the nature of the substituent.^{7,8}

Alkyl substitutions favor CO cleavage both photochemically and thermally. In the latter case, the experimental activation energy is around 52 kcal/mol. The CC rupture involves an activation energy which is 5–7 kcal/mol higher. Moreover, the corresponding intermediate has been trapped by solvent capture in the case of a photochemical reaction.

Aryl substitutions conversely favor CC breaking which yields 1,3-dipolar species as primary products.^{4b} These ylides have been characterized at low temperature (77 K) in solid matrix.^{10a} A preferentially disrotatory mode of opening is observed in the photochemically induced reaction. By further evolution, the dipolar intermediate can be trapped in some occurrences, or, more generally, affords a carbenic species and a carbonyl compound.^{10b}

The general scheme of Figure 1 provides a basis for a rationale of the experimental results: opening of the cycle via a one-bond rupture (CO rupture, path 1, and CC rupture, path 2) yields two different intermediates (I and II). Cycle breaking by a simultaneous two-bond rupture leads either to the formation of ethylene and atomic oxygen (path 3) or formaldehyde plus a carbenic methylene (path 4). The latter fragments

can also proceed from evolution of the intermediates I, by CC rupture (path 6), or II, by CO rupture (path 5), and the former from intermediate I by CO rupture (path 8). At least, the intermediate I can, by hydrogen migration from one carbon to the other, afford acetaldehyde (path 8).

In order to get some new insight on the intimate mechanisms of these different reactions, all these paths have been theoretically simulated taking ethylene oxide as a model structure. In this first paper, we will limit ourselves to the study of the formation of intermediates I and II according to paths 1 and 2.

The potential energy curves (PECs) of the various electronic states under consideration were obtained by ab initio SCF-CI calculations, following a previously described method,^{11b} using the STO-3G basis set¹² of the GAUSS 70 series of programs.¹³ The CI segment was carried out on a selection of the first 100 mono- or biexcited configurations, formed by the promotion of one or two electrons from the six highest occupied to the four lowest unoccupied MOs.^{11c} In this study, the reaction coordinate is the opening angle of the cycle; all the other geometrical parameters are assumed to follow linear variations between their initial and final values.¹⁴

This technique, associated with the small size of the basis set and the limited CI, does not lead to precise quantitative information such as vertical excitations or energy barriers. Nevertheless, keeping these limits in mind, the method is well suited to get semiquantitative information of chemical significance, as already illustrated by other studies in related fields.^{11b}

Oxirane Calculated Properties

We have adopted in this study the STO-3G geometry calculated by Pople et al.,¹⁵ which is in good agreement with experimental determinations¹⁶ as well as other calculations.¹⁷

The first calculated singlet vertical excitation ($^1A_2 = ^1n_zW_A^*$)¹⁸ lies at 123.7 nm (10.03 eV) and the corresponding triplet, 3A_2 , at 129.8 nm (9.55 eV). Then come two quasi-degenerate triplet states ($^3B_1 = ^3n_zW_s^*$, $^3B_2 = ^3n_xW_A^*$) at 117.7 (10.48 eV) and 117.2 nm (10.52 eV), respectively, and next, a degenerate singlet-triplet pair ($^1B_1, ^3A_1$) at 100.2 nm (12.3 eV).

Experimental values are difficult to determine, owing to the presence in the valence transition region of Rydberg transitions.¹⁹ Basch et al.^{19a} estimate that the 7.24-, 7.89-, and 8.64-eV bands correspond to Rydberg absorptions, and that the 9.05- and 10.41-eV ones correspond to the first valence excitations, but this assignment is not fully ascertained. The only clear fact is the position of the first ionization potential at 10.57 eV.^{19a,20}

A word of caution must be added regarding the role of Rydberg excitations. At the present time, it is not clear whether these states intervene or not in usual photochemical processes,

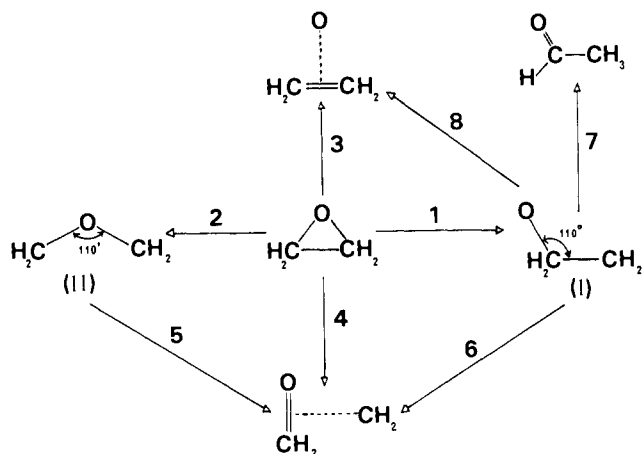


Figure 1. Scheme presenting different possible reaction paths for the oxirane molecule. In this study, only path 1 and path 2 are studied.

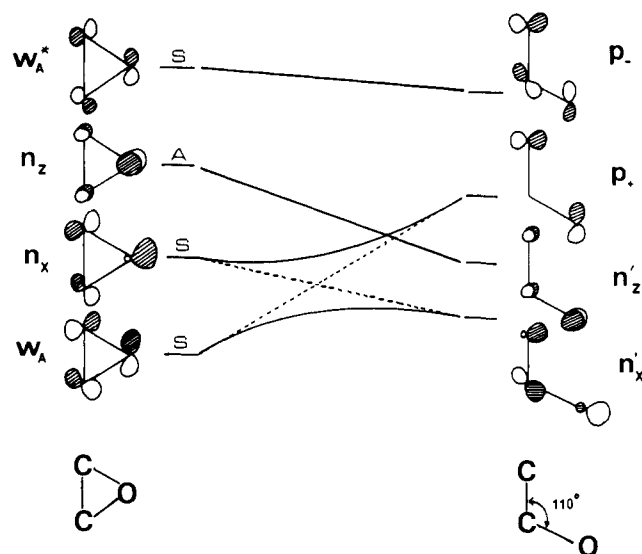


Figure 2. CO bond rupture leading to the open intermediate I, path 1: MO correlation diagram. The symmetry symbols S or A refer to the OCC plane which is preserved in the process.

and further studies are needed in this field. In ethylene oxide, the low-lying Rydberg states are related to the 3s orbital of the oxygen atom. These states might be counted as potentially low energy reservoirs, able to cross the reactive PECs along a given reaction path. But their high diffuseness should involve two main consequences: they should not interact specifically with a special part of the bonding framework, and the electronic flow from them to the valence states is not expected to be very efficient. In other words, we suppose to a first approximation that their presence would not alter significantly the classical picture of reactivity based on the analysis of valence states.

The values of the chemically active irradiation energies determined by Kawasaki et al.^{4a} (147 nm or 8.39 eV and 174 nm or 7.09 eV) thus appear in the Rydberg range and do not allow a precise determination of the position of the first vertical valence excitation. Thus, in spite of our limited calculations, our values appear as realistic upper limits of the real ones.

The positions of the different molecular orbitals (MOs) are in full agreement with other calculations using a more extended basis.²⁰ They are pictured in Figure 2 and will be of crucial interest in all the following discussions.

CO Cleavage (Path 1)

To simulate this evolution, oxirane was progressively transformed into I. The structure of this intermediate²¹ is

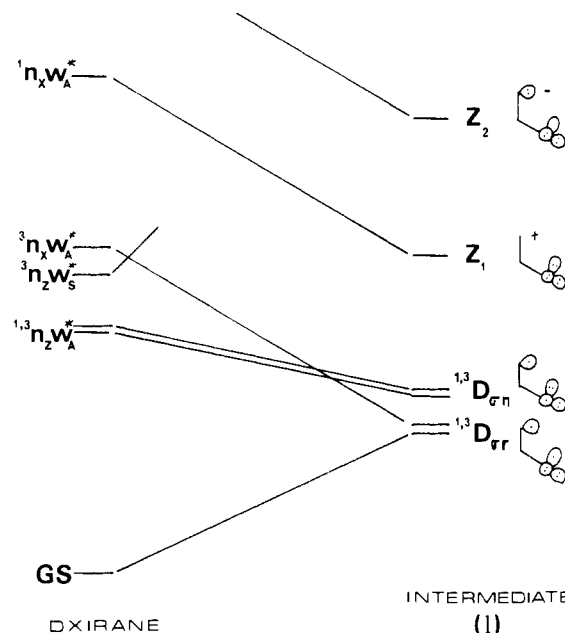


Figure 3. State correlation diagram corresponding to the CO bond rupture (path 1).

Table I. Relative Importance of the Primary Photolytic Processes in Oxirane

primary products ^a	147.0 nm	174.4 nm	178.3-184.5 nm	253.7 nm Hg (³ P)	pyrolysis 450 °C
CH ₃ · + HCO·	1.0	1.0	1.0	1.0	1.0
O + C ₂ H ₄	0.7	0.2	0.1	0.1	trace
H ₂ + CH ₂ CO	0.1	0.1		0.1	
CH ₃ CHO	0.2			0.7	
CH ₂ + CH ₂ O	0.2			trace	

^a Reference 4c.

characterized by a 110° value of the OCC angle²² and the symmetrical location of the terminal methylene with respect to the OCC plane. It has been verified that this situation is energetically more favorable than the corresponding one in which the two hydrogens are in the OCC plane ($\Delta E = 3$ kcal/mol).

In Figure 2 is drawn the MO correlation diagram, whose main features are the following: on the one hand, the two oxygen lone pairs of oxirane, called n_z and n_x , intend initially to preserve their identity and to reach n_z' and n_x' , the two lone pairs of the product. On the other hand, the two antisymmetric Walsh orbitals,²³ the bonding one W_A and the antibonding W_A^* , tend to transform into the quasi-degenerate couple p_-/p_+ , corresponding respectively to the out of phase and in-phase combinations of the in-plane lobes centered on the atoms of the broken bond. Consequently, the intended correlation lines (dashed lines) would cross, but for symmetry reasons these crossings are avoided and the observed correlations (full lines) link W_A to n_x' and n_x to p_+ . Corresponding to this MO diagram, the state correlations are drawn in Figure 3.

Let us first describe the various electronic states of intermediate I.

The shape and the energetic position of the MO couple p_-/p_+ allow us to consider I as an homsymmetric diradical.²⁴ Indeed its ground state (GS) is a covalent diradical $^1D_{\sigma\sigma}$ corresponding to the location of the two upper electrons in p_- and p_+ . It is contaminated by some ionic character arising from the dissymmetry of the system. Degenerate in energy is the purely covalent triplet $^3D_{\sigma\sigma}$. In close vicinity are the singlet-triplet states $^{1,3}D_{\sigma\sigma}$ corresponding to the promotion of one electron

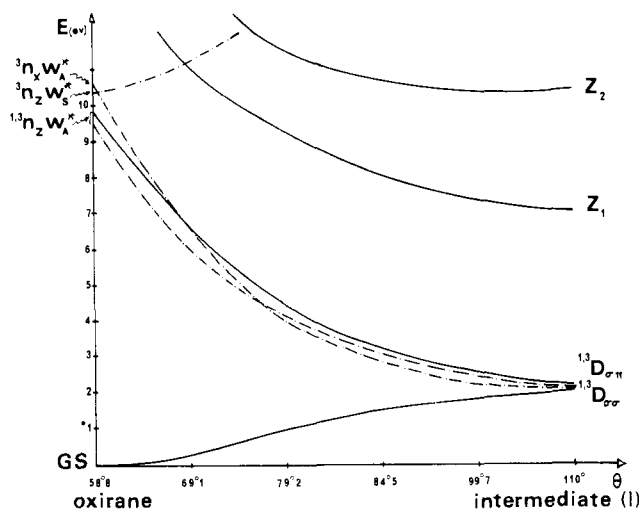


Figure 4. Calculated PECs for the CO bond rupture (path 1). θ refers to the OCC angle. The dotted lines are relative to the triplet and the full lines to the singlet states. The calculated points are indicated in abscissas.

from n_z' (π plane) into the p_-/p_+ couple (σ plane). The first ionic state Z_1 lies more than 4.5 eV above.

The state correlation diagram is straightforward. The initial GS is linked to ${}^1D_{\sigma\sigma}$ while ${}^3D_{\sigma\sigma}$ comes from ${}^3n_x W_A^*$. The singlet-triplet pair ${}^{1,3}n_z W_A^*$ transforms naturally into the ${}^{1,3}D_{\sigma\pi}$ pair of states while Z_1 comes from the high-lying ${}^1n_x W_A^*$. No avoided crossing intervenes there. The calculated PECs (Figure 4) confirm this analysis. The dominant features are the following.

(1) There is no maximum on the GS PEC, in full agreement with the fact that there is no HOMO-LUMO crossing at the MO level. Thermal ring opening necessitates an activation energy of 45 kcal/mol, and, since no extremum appears along this reaction coordinate, the open form is likely to reclose spontaneously to give the initial molecule, except if another reaction path can compete with this opportunity.

(2) The slopes of the first excited singlet and triplet PECs are descending fast and monotonically, and, consequently, direct irradiation or adequate sensitization will lead to the same cleavage.

(3) The singlet-triplet degeneracy (${}^{1,3}D_{\sigma\sigma}, {}^{1,3}D_{\sigma\pi}$) of the different states of the intermediate I can lead to easy inter-system crossings²⁵ or internal conversions. This situation would considerably lower the effective yield of the opening reaction since a leak exists to allow re-formation of the initial system from the open form.

We must note that, if only a part of the total energy is dissipated with the neighborings, intermediate I would possess a considerable amount of internal energy (maximum 6 eV), able to initiate a further evolution of the system (fragmentation) as will be seen later.

CC Cleavages

Following Woodward-Hoffmann considerations,²⁶ a number of works have been devoted to the different modes of opening of the three-membered rings.²⁷ We encounter here the same type of problems and, as in previous studies, we will distinguish three typical modes: the face to face (FF) mode which preserves two orthogonal symmetry planes; the conrotatory mode which preserves a C_2 axis; the disrotatory mode which preserves only the symmetry plane perpendicular to the COC plane.

In the last two cases, the same final form, edge to edge (EE), is obtained.

Face to Face Cleavage. The final structure of the intermediate II reached at the end of the process is essentially char-

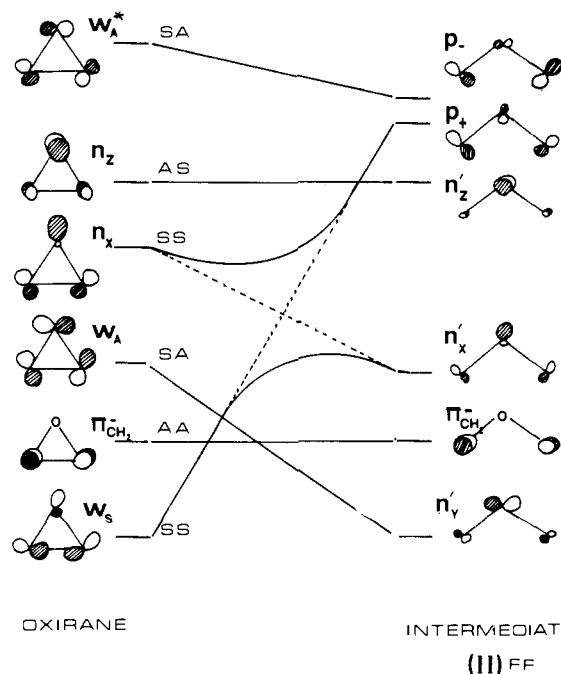


Figure 5. MO correlation diagram corresponding to the face to face CO bond rupture leading to the intermediate II (FF), path 2. The symmetry symbols refer first to the COC plane and second to the perpendicular plane, which are both preserved in the opening process.

acterized by the 110° value of the COC angle and the orientation of the two extreme methylenes, orthogonal to the COC plane.²⁸

The MO correlation diagram corresponding to this rupture is depicted in Figure 5. Guided by symmetry considerations, the first index refers to the xOy plane and the second to the xOz plane. Most correlations are straightforward and only the SS couple of MOs deserves any comments. n_x initially intends to correlate with its counterpart n_x' and W_S with p_+ , in-phase combination of the lobes centered on the carbon atoms. This situation leads to an avoided crossing at the SCF level and finally n_x correlates with p_+ and W_S with n_x' (full lines).

The quasi-degenerate pair of MOs, p_- and p_+ , in II is well suited to allow the now classical description of a homosymmetric diradical. Its first electronic states are the mainly covalent ${}^{1,3}D_{\sigma\sigma}$ forms. Next comes the first ionic state Z_1 , which is negative mixing of the two charged resonance forms. Slightly above are the ${}^{1,3}D_{\sigma\pi}$ states, which correspond to the promotion of one electron from the n_z' lone pair to the MO couple p_-/p_+ . The state correlations are simple as indicated in Figure 6. All the crossings are allowed since the concerned states have different symmetries or multiplicities. In Figure 7 are drawn the calculated PECs.

The ${}^1D_{\sigma\sigma}$ diradical lies at 83 kcal/mol above oxirane GS. This clearly states that the thermal CC cleavage is much less probable than the CO one (45 kcal/mol). As in the cyclopropane case, and after the MO and state correlation diagrams considerations, the ${}^1D_{\sigma\sigma}$ state of II is reached from oxirane GS without passing through an energy maximum. As a consequence, the open intermediate II is likely to reclose spontaneously to regenerate the initial structure. Photochemical reactivity notably differs from that of the CO cleavage. As previously, the initial state leading to ${}^3D_{\sigma\sigma}$ of II is ${}^3n_x W_A^*$, but this time the ${}^{1,3}n_z W_A^*$ couple is not so easily reactive. Indeed, the two possible reactive paths are not direct. The first one consists in reaching the ${}^3D_{\sigma\pi}$ form, remaining on the ${}^3n_z W_A^*$ PEC. This channel involves an energy increase of around 10 kcal/mol. Accumulation of this extra energy is possible considering the estimated lifetime of a triplet state,^{11b} if no other

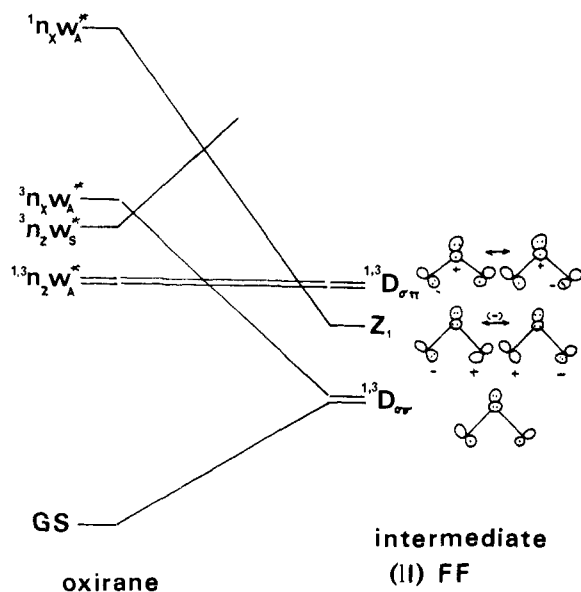


Figure 6. Face to face CC bond rupture (path 2): state correlation diagram.

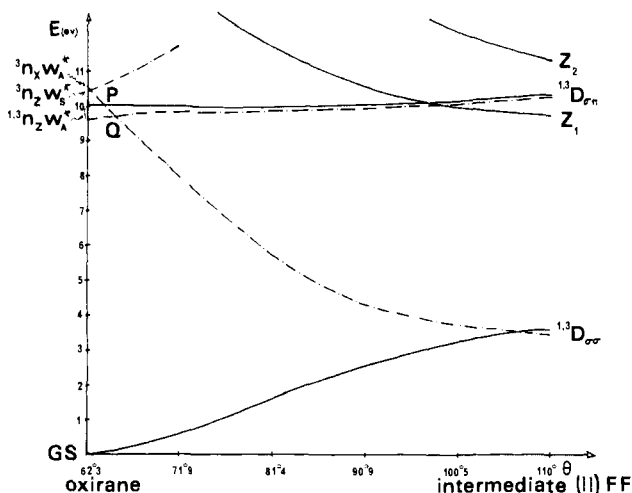


Figure 7. Calculated PECs for the CC bond rupture according to path 2. θ refers to the COC angle. The dotted lines are relative to the triplet and the full lines to the singlet states. The calculated points are indicated in abscissas.

competitive reaction pathway intervenes. The second possibility consists in reaching the dissociative ${}^3n_x W_A^* \leftrightarrow {}^3D_{\sigma\pi}$ PEC via a favorable intersystem crossing from the singlet ${}^1n_z W_A^*$ (point P) or through an internal conversion from the triplet ${}^3n_z W_A^*$ (point Q). Thus the easiest ways to obtain the face to face cleavage are direct population of ${}^3n_x W_A^*$ by sensitization or favorable intersystem crossing between the first populated singlet and the dissociative PEC.

Conrotatory and Disrotatory CC Cleavages. The common final structure is the edge to edge (EE) planar form of intermediate II. The COC angle was here again fixed at 110° . The similitude with the isoelectronic allyl anion brings with it that energy and electronic distribution strongly depend on CO bond length variations. When this bond length is 1.433 \AA (nonrelaxed structure), the CO Mulliken population is 0.22 and the antibonding π_3 is the HOMO (see Figure 8). When this distance is 1.36 \AA (standard value²⁹), the CO Mulliken population is 0.34 and the HOMO is the nonbonding π_2 MO. These changes are closely related to the familiar resonance picture. When the CO bonds are shortened, the weight of charged resonance forms is increased. This is clearly illustrated by the

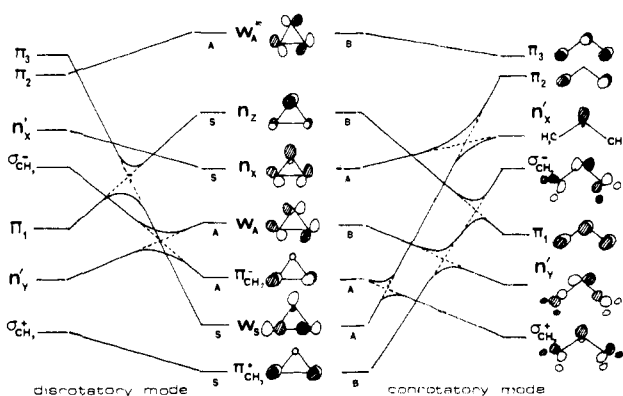


Figure 8. MO correlation diagrams for the disrotatory (left side) and the conrotatory (right side) CC bond rupture of oxirane leading to the intermediate II (EE). The symmetry symbols A and S (left), A and B (right), refer to the symmetry elements which are preserved during the processes (a plane in the disrotatory mode, a C_2 axis in the conrotatory mode).

nature of the singlet GS of the EE intermediate II: for a long CO bond (1.433 \AA), the eigenstate is roughly 0.25 ionic + 0.75 covalent, while at 1.36 \AA , it is 0.33 ionic + 0.67 covalent.³⁰ The latter form is favored by a 5 kcal/mol energy difference.

The calculated MO correlation diagrams corresponding to these two modes are depicted in Figure 8 (left side for the disrotatory process, right side for the conrotatory one). In order to determine the natural correlations, two main considerations apart from symmetry labeling can be invoked. First, it appears that, if we consider the two main distortions occurring during this process, i.e., CC bond lengthening and CH_2 rotation, the methylene motion dictates the behavior of the MOs centered on these fragments. Secondly, the MOs mainly centered on oxygen tend to correlate with their counterparts since they are not severely affected by the motion. Then, in the disrotatory as well as in the conrotatory process, n_z tends to naturally correlate with π_1 , n_x with n_x' , and W_A with n_y' .

During the disrotatory process, $\pi^+_{CH_2}$ tends to correlate with $\sigma^+_{CH_2}$, W_S with π_3 , $\pi^-_{CH_2}$ with $\sigma^-_{CH_2}$, and W_A^* with π_2 . Two avoided crossings result (dashed lines) and a HOMO-LUMO crossing appears for a COC angle of 95° . This situation is characteristic of a thermal forbidden process according to Woodward-Hoffmann's terminology.²⁶

In the conrotatory process, $\pi^+_{CH_2}$ tends to correlate with $\sigma^-_{CH_2}$, W_S with π_2 , $\pi^-_{CH_2}$ with $\sigma^+_{CH_2}$, and W_A^* with π_3 . Various crossings occur between occupied MOs but none between HOMO and LUMO. There is therefore a drastic difference with the disrotatory process. Let us now examine the consequences in the state correlations.

In a first step, we will consider the different electronic configurations of the common open structure EE (II). The first singlet ${}^1D_{\pi\pi}$, whose eigenstate is $0.87(\pi_2)^2 - 0.48(\pi_3)^2$, depicts a homosymmetric diradical. It is nearly degenerate with the corresponding triplet ${}^3D_{\pi\pi}$. Next come the zwitterionic singlets Z_1 and Z_2 whose electronic configurations are respectively ${}^1(\pi_2\pi_3)$ and $0.42(\pi_2)^2 + 0.72(\pi_3)^2$; the ultimate states we will consider are the ${}^{1,3}D_{\sigma\pi}$ pair. They correspond to the configuration ${}^{1,3}(\sigma^-_{CH_2} \rightarrow \pi_3)$.

According to the MO diagram, the following state correlations are straightforward in the disrotatory process: ${}^1n_z W_A^* \rightarrow Z_1$, ${}^3n_z W_A^* \rightarrow {}^3D_{\pi\pi}$, ${}^{1,3}n_x W_A^* \rightarrow {}^{1,3}D_{\sigma\pi}$. In the conrotatory process they become ${}^{1,3}n_z W_A^* \rightarrow {}^{1,3}D_{\sigma\pi}$, ${}^1n_x W_A^* \rightarrow Z_1$, and ${}^3n_x W_A^* \rightarrow {}^3D_{\sigma\pi}$ (see Figure 9).

In both cases, the main difficulty is to determine which oxirane state ${}^1D_{\pi\pi}$ and Z_2 come from, since these states are mixtures of the two $(\pi_2)^2$ and $(\pi_3)^2$ configurations as previously seen. According to the MO diagram, $(\pi_2)^2$ correlates with oxirane ground state in the conrotatory process, while it correlates with a doubly excited state in the disrotatory one.

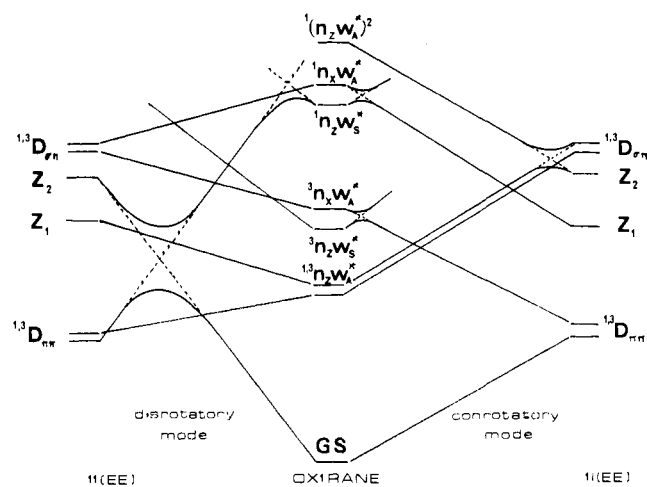


Figure 9. State correlation diagram for the disrotatory (left) and the conrotatory (right) modes of CC bond rupture, leading to the common EE form of the intermediate II.

Conversely $(\pi_3)^2$ correlates with oxirane ground state in the disrotatory process and with $(n_x)^2$ in the conrotatory one. Consequently, according to this scheme there is an avoided crossing at state level in the disrotatory mode, while there is none in the conrotatory mode. However, the mixing of these two configurations leading to ${}^1D_{\pi\pi}$ and Z_2 cuts down considerably this difference. Indeed, in both cases, the corresponding correlation lines, owing to the mixing, will repel each other at the end of the process (when the mixing is maximum). Thus, in both cases, the GS PEC will not remain monotonous, the maximum being more pronounced in the disrotatory process.

The state correlation diagram of Figure 9 illustrates all these comments and the calculated PECs of Figures 10 and 11 are in full agreement with the preceding analysis.

The dominant features are the following.

(1) The barriers on the GS PEC are 3.8 (conrotatory) and 4.1 eV (disrotatory). Consequently, the conrotatory mode is thermally favored. The experimental findings are in good agreement with this result.^{4b} To reclose, the open form II in its ${}^1D_{\pi\pi}$ state necessitates a 0.4- and 0.7-eV activation energy in the conrotatory and disrotatory mode, respectively. Thus, we can estimate that the intermediate lives long enough to be trapped or to pursue some other evolution since it behaves in a true potential well.

(2) If we consider oxirane excited in its first singlet, ${}^1n_zW_A^*$, it can either lead directly to the Z_1 state of the open form in a disrotatory process or, after a favorable intersystem crossing at point C, lead to the ${}^3D_{\pi\pi}$ state in a conrotatory process, unless it decays by internal conversion to ${}^3n_zW_A^*$.

(3) In this excited form the system directly evolves toward the ${}^3D_{\pi\pi}$ state of the intermediate II in a disrotatory motion. The PECs crossings at R and S can lower the efficiency of the whole process since they provide a possible return to the oxirane GS.

Comparison of the Different Ring Openings

Comparing Figures 4, 7, 10, and 11, we can draw some conclusions. Let us first consider thermal reactivity.

The smallest energetical barrier from oxirane GS to the open forms I and II is found in the CO cleavage (2 eV). All the CC rupture modes require a higher activation energy: 3.6 eV for the face to face process, 3.8 eV for the conrotatory mode, and 4.1 eV for the disrotatory one. However, the open form I, in its ${}^1D_{\sigma\sigma}$ state, does not constitute a real intermediate since no barrier prevents it from reclosing to oxirane, unless some competing process can take place. Although CO cleavage

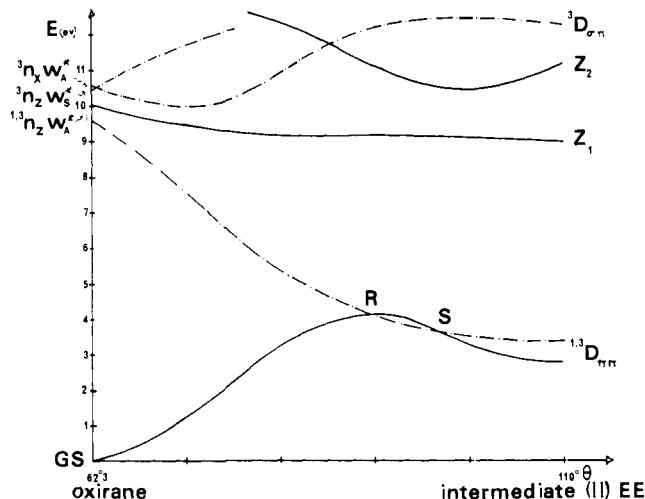


Figure 10. Calculated PECs corresponding to the disrotatory CC bond rupture. θ refers to the COC angle. The dotted lines are relative to the triplet and the full lines to the singlet states. The calculated points are indicated in abscissas.

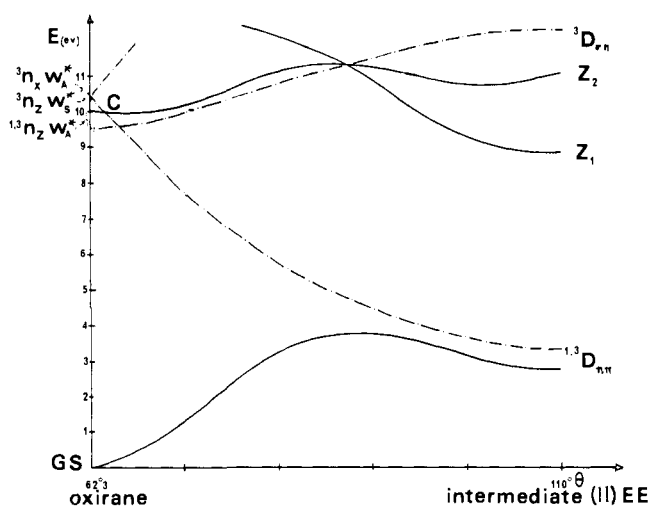


Figure 11. Calculated PECs corresponding to the conrotatory CC bond rupture. θ refers to the COC angle. The dotted lines are relative to the singlet states. The calculated points are indicated in abscissas.

appears as the easiest, it cannot be very efficient in the ground state.

Considering now the GS PECs slopes during the CC cleavages, one can estimate that the opening would begin with a CC bond lengthening which is rather face to face, up to $\theta \approx 90-100^\circ$; then the motion would end up with a CH_2 groups rotation to yield the open form II in its EE geometry, 2.8 eV above the initial GS. This process, although more difficult than CO cleavage, leads to an intermediate which can be trapped or undergo further evolution.

Now, let us consider photochemical reactivity. Clearly, the easiest and most efficient pathway appears to be CO cleavage, whether in the ${}^1n_zW_A^*$ or in the ${}^3n_zW_A^*$ state. In the singlet state, two less probable, but competitive, processes are CC cleavages in the face to face or conrotatory motion. Both need an effective intersystem crossing and lead to the ${}^3D_{\pi\pi}$ state of the open form II. One last possibility is the formation of the Z_1 ionic form, of high energy, by a disrotatory motion.

In the triplet state, only the disrotatory opening—leading to the ${}^3D_{\pi\pi}$ state of II—can compete.

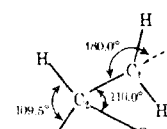
In all cases of a photochemical process, the open forms I and II, in their ${}^1,3D_{\sigma\sigma}$ or ${}^1,3D_{\pi\pi}$ states, possess a large energy excess which can serve to overcome the activation barriers of subsequent reaction steps.

All these conclusions are in agreement with experimental results: CO cleavage is indeed the easiest reactive path for alkyl-substituted oxiranes, although some other competing processes exist. For aryl-substituted structures, an important modifying factor intervenes: the zwitterionic forms are strongly stabilized. Thus, the slope of the ${}^1n_2W_A^* \rightarrow Z_1$ PEC, in the disrotatory CC cleavage, will be steeper and this mode can then compete with CO opening. This fact will be experimentally enhanced since II in its Z_1 state cannot reclose to oxirane while I in its lower state ${}^1D_{\sigma\sigma}$ can do it spontaneously; as a consequence, II can be the major primary stable product detected. This conclusion is in agreement with the fact that II gives easy 1,3-dipolar cycloaddition products, contrary to I.^{4b}

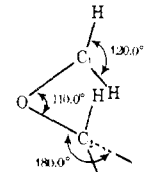
In this paper we have limited ourselves to the study of the primary processes leading to the open forms. Their evolution will be analyzed in the accompanying paper.

References and Notes

- (1) For preceding paper, see B. Bigot, A. Sevin, and A. Devaquet, *J. Am. Chem. Soc.*, **100**, 6924 (1978).
- (2) This laboratory is associated with CNRS (ERA no. 549).
- (3) For a review, see J. March, "Advanced Organic Chemistry", McGraw-Hill, New York, N.Y., 1968; N. L. Allinger et al., "Organic Chemistry", Worth Publishers, New York, N.Y., p 441.
- (4) (a) M. Kawasaki, T. Ibuki, M. Inasaki, and Y. Takesaki, *J. Chem. Phys.*, **59**, 2076, 6321 (1973); (b) R. Huisgen, *Angew. Chem., Int. Ed. Engl.*, **16**, 572 (1977), and references cited therein; (c) S. Braslavsky and J. Hecklen, *Chem. Rev.*, **77**, 4473 (1977), and references cited therein.
- (5) (a) R. Gomer and W. A. Noyes, *J. Am. Chem. Soc.*, **72**, 101 (1950); (b) N. R. Bertoniere and G. W. Griffin, "Organic Photochemistry", Vol. II, O. L. Chapman, Ed., Marcel Dekker, New York, N.Y., 1973, Chapter 2, and references cited therein.
- (6) (a) M. L. Neufeld and A. T. Blades, *Can. J. Chem.*, **41**, 2956 (1963); (b) S. W. Benson, *J. Chem. Phys.*, **40**, 105 (1964).
- (7) R. J. Cvetanovic and L. C. Doyle, *Can. J. Chem.*, **35**, 605 (1957); M. C. Flowers, R. M. Parker, and M. A. Voisey, *J. Chem. Soc. B*, 239 (1970).
- (8) M. C. Flowers and D. E. Penny, *J. Chem. Soc., Faraday Trans. 1*, **70**, 355 (1974); T. Do Minh, A. M. Trozollo, and G. W. Griffin, *J. Am. Chem. Soc.*, **92**, 1402 (1970); G. A. Lee, *J. Org. Chem.*, **41**, 2656 (1976).
- (9) H. Christinson, R. A. Mater, and G. W. Griffin, *Chem. Commun.*, 415 (1966).
- (10) (a) R. S. Becker, R. O. Bost, J. Kolc, N. R. Bertoniere, R. C. Smith, and G. W. Griffin, *J. Am. Chem. Soc.*, **92**, 1302 (1970); (b) G. W. Griffin, *Angew. Chem., Int. Ed. Engl.*, **10**, 537 (1971).
- (11) (a) A. Devaquet, *Top. Curr. Chem.*, **54**, 1 (1975). (b) B. Bigot, A. Sevin, and A. Devaquet, *J. Am. Chem. Soc.*, **100**, 2639 (1978). (c) In this procedure, all the valence states that matter for the study of reactivity are properly correlated in most cases. When a HOMO-LUMO crossing occurs, triply excited states are necessary to correlate some monoexcited states of the starting molecule. Referring ourselves to previous calculations on parent systems, the addition of triply excited states does not significantly alter the calculated energies of the reactive states under examination. Triply excited configurations were thus discarded in this study.
- (12) W. J. Hehre, R. F. Stewart, and J. A. Pople, *J. Chem. Phys.*, **51**, 2657 (1969).
- (13) W. J. Hehre, W. A. Lathan, R. Ditchfield, M. D. Newton, and J. A. Pople, QCPE, No. 236, Indiana University, Bloomington, Ind.
- (14) We have assumed standard bond lengths and angles for the final structures.
- (15) W. A. Lathan, R. Radom, P. C. Hariharan, W. J. Hehre and J. A. Pople, *Top. Curr. Chem.*, **40**, 1 (1973).
- (16) G. L. Cunningham Jr., W. A. Boyd, R. J. Myers, W. D. Gwinnand, and W. I. Levan, *J. Chem. Phys.*, **19**, 676 (1951); R. C. Lord and B. Nohn, *ibid.*, **24**, 656 (1956).
- (17) (a) D. T. Clark, *Theor. Chim. Acta*, **15**, 225 (1969); (b) R. Bonaccorsi, E. Scrocco, and J. Tomasi, *J. Chem. Phys.*, **52**, 5270 (1970).
- (18) The molecule lies in the xOy plane.
- (19) (a) H. Basch, M. B. Robin, N. A. Kubler, C. Baker, and D. W. Turner, *J. Chem. Phys.*, **51**, 52 (1969); (b) T. K. Liu and A. B. F. Duncan, *ibid.*, **17**, 241 (1949); A. Lowry III and K. Watanabe, *ibid.*, **28**, 208 (1958); (c) D. H. Anc, H. M. Webb, and M. T. Bowers, *J. Am. Chem. Soc.*, **97**, 4137 (1975).
- (20) W. von Niessen, L. S. Cederbaum, and W. P. Kraemer, *Theor. Chim. Acta*, **44**, 85 (1977).
- (21)



$C_1C_2 = 1.52 \text{ \AA}$
 $C_2O = 1.43 \text{ \AA}$
 $HC_1H = 120^\circ$
 $OC_2C_1 = 110^\circ$
- (22) This value corresponds to a realistic CO elongation and represents a classical valence angle for a tetravalent carbon atom.
- (23) They are so named by analogy with cyclopropane.
- (24) L. Salem and C. Rowland, *Angew. Chem., Int. Ed. Engl.*, **11**, 92 (1972).
- (25) M. A. El Sayed, *J. Chem. Phys.*, **38**, 2834 (1963); Sheng Hsien Lin, *ibid.*, **44**, 3759 (1966); T. S. Lee, *J. Am. Chem. Soc.*, **99**, 3909 (1977).
- (26) R. B. Woodward and R. Hoffmann, *Angew. Chem., Int. Ed. Engl.*, **8**, 781 (1969).
- (27) R. Hoffmann, *J. Am. Chem. Soc.*, **90**, 475 (1968); P. J. Hay, W. J. Hunt, and W. A. Goddard III, *ibid.*, **94**, 638 (1972); J. A. Horsley, Y. Jean, C. Moser, L. Salem, M. Stevens, and J. S. Wright, *ibid.*, **94**, 279 (1972); Y. Jean and X. Chapuisat, *ibid.*, **96**, 6911 (1974); A. K. Q. Siu, W. M. StJohn, and E. F. Hayes, *ibid.*, **92**, 7249 (1970); E. F. Hayes and A. K. Q. Siu, *ibid.*, **93**, 2090 (1971); D. R. Arnold and L. A. Karnischky, *ibid.*, **92**, 1404 (1970); R. J. Buenker and S. D. Peyerimoff, *J. Phys. Chem.*, **73**, 1299 (1969).
- (28)



$OC_1 = OC_2 = 1.43 \text{ \AA}$
 $C_1OC_2 = 110^\circ$
 $HCH = 120^\circ$
- (29) W. J. Hehre, W. A. Lathan, and J. A. Pople, *J. Am. Chem. Soc.*, **89**, 4253 (1967). The optimization of the CO bond length (GS) only affords an energy gain of 1.8 kcal/mol to our standard structure. The optimal CO distance is 1.325 Å.
- (30) Calculated according to ref 24.